The influence of C2H2 and dust formation on the time dependence of metastable argon density in pulsed plasmas

Ilija Stefanovic, Nader Sadeghi, Jörg Winter

The influence of C_2H_2 and dust formation on the time dependence of metastable argon density in pulsed plasmas

Ilija Stefanović[1, 2], Nader Sadeghi[3] and Jörg Winter[1]
[1]Institut für Experimentalphysik II, Ruhr-Universität Bochum, 44780 Bochum, Germany
[2]At leave of absence from Institute of Physics, Belgrade University, 11080 Belgrade, Serbia
[3]Laboratoire de Spectrometrie Physique, University Joseph Fourier and CNRS, Grenoble, France

E-mail: Ilija.Stefanovic@rub.de

Abstract: Diode laser absorption at 772.38 nm is used to measure the time resolved density of Ar*($^3P_2$) metastable atoms in a capacitively coupled radio-frequency (RF) discharge running in argon/acetylene mixture at 0.1 mbar. The RF power is pulsed at 100 Hz and the density of Ar*($^3P_2$) atoms in the 5 ms ON time and in the afterglow are recorded. Different plasma conditions, namely: 1) pure argon, 2) argon + 7% acetylene before powder formation, 3) argon + 7% acetylene after dust particles have been formed and 4) argon with dust particles remained in the plasma volume but without acetylene are studied. The measured steady-state Ar*($^3P_2$) density in the middle of the reactor is always about 10 times larger in dusty argon plasma than in pure argon discharge. This is mainly a consequence of the enhancement of electron temperature after dust formation. Both steady state densities and decay times in the afterglow indicate that the degree of dissociation of C_2H_2 in the plasma volume can be as high as 99%. It is shown that in our plasma conditions on the surface of dust particles the loss of Ar*($^3P_2$) atoms is negligible compared to their loss by diffusion to the electrodes.

PASC: 52.25.b, 52.27.Lw, 52.70.Gw, 52.70.Kz

1. Introduction

Basic properties and application of dusty plasmas (plasmas containing nano- to micro-sized particles) have been discussed by many authors in the literature [1]. Especially, the change in plasma properties by immersing or growing dust particles in plasma was addressed. Experimental results showed that if the dust particle density was sufficiently large, the important electron loss on these particles leads to a significant decrease of electron density. This forces the plasma to "respond" by increasing the electron production rate, obtained by an enhancement of the electron temperature [2,3,4]. Important changes on electrons temperature and density, as well as on optical emission properties have been reported [5, 6,7,8,9]. Also, the dusty plasma models predicted differences in behaviour when comparing dusty and dust free plasmas, like change in phase shift between voltage and current (α-γ transition) [10] or different power deposition and electron energy distribution [11-13].

Argon metastable atoms (Ar*) have been used to investigate the kinetics of fast electrons in numerous discharge configurations [14-17]. These atoms also served as a probe to monitor the kinetic energy of heavy particles in the plasma, deduced from the Doppler profile of an absorption line [18-20]. Recently, the density of Ne* in neon with dust particles immersed [21] and of Ar* in argon/acetylene with plasma-polymerized dusts has been analyzed [22]. However, the kinetics of Ar* metastables in the afterglow of a pulsed complex plasma have not yet been investigated. Pulsing the radiofrequency (RF) discharge permits to control the generation of dust particles in reactive plasmas [23]. It was found [24] that by varying the pulsed frequency and duty cycle the dust particle nucleation could be increased or suppressed. So, it is of prime importance to understand the basic properties of dusty plasma afterglow, in particular the behaviour of Ar* metastables who posses about 11.5 eV of internal energy and can initiate chemical reactions in the afterglow or induce electron detachment from negatively charged dust particles.

To measure the Ar* density and its time behaviour, we used the Laser Absorption Spectroscopy (LAS) on argon $^3P_2$ metastable state. The details of the experimental technique are given in the following paragraph and results relative to the time dependence of metastable density during the RF pulse and in the afterglow for different plasma conditions are analyzed and discussed in the last paragraph. With a fixed RF power, we have considered four different situations: 1- pure argon plasma (Ar); 2- argon/acetylene plasma before dust formation (Ar/C_2H_2); 3- argon/acetylene plasma after dust particles have been formed and grown to reach a steady-state (Ar/C_2H_2/dust); 4- after step 3, the plasma is maintained running but the acetylene flow is stopped. This way, dust particles remain inside "pure" argon plasma (Ar/dust).

2. Experiment

The detail of plasma chamber used in this work to generate the plasma has been described elsewhere [25]. The capacitively coupled (CCP) symmetrically driven radio-frequency (RF) 13.56 MHz discharge is produced by two parallel-plane 30 cm diameter electrodes located inside a 50 cm diameter 30 cm high stainless steel cylinder chamber. The electrode gap, which can be varied externally, was fixed to 7.0 cm in these experiments. The discharge was driven in cw or pulse modes, with variable pulsing frequency between 100 Hz and 1 kHz. Most results reported in this paper have been obtained at 100 Hz. Pure argon (8 sccm) or with 0.5 sccm C_2H_2 mixture was supplied to the discharge chamber and a throttle valve in the exit port kept constant the gas pressure at 0.1 mbar. The discharge input power ranged between 10 W and 80 W and for each plasma condition the match box was adjusted to keep the reflected power to less than a few percent of the forward power. The carbonaceous nano-particles (dust) have been formed in the process of plasma polymerization of acetylene monomer [25,26]. To follow the time variation of Ar*($^3P_2$) metastable atoms, we have employed the laser absorption spectroscopy (LAS) technique on 772.38 nm argon line ($1s_5$-$2p_7$ transition in Paschen notation [27]), described in [28]. The light source was an external cavity single mode diode laser, ECDL (Sacher Lasertechnik), whose width (<10 MHz) was much smaller than the typical bandwidth of the absorption line (≅0.8 GHz). The laser frequency could be finely and accurately scanned by changing the voltage on the piezoelectric element that moved one of the cavity mirrors. The beam from the ECDL was split in three parts with beam splitters. A first beam was guided to a 20 cm long confocal Fabry-Perot interferometer (375 MHz free spectral range) and detected with a photodiode PD1, to perform precise laser frequency calibration. The 2nd beam crossed a low pressure low current argon discharge tube and then detected with a photodiode PD2. It served for the absolute scale

frequency calibration of the laser [28]. The last beam, attenuated down to <10 μW, by a set of neutral density filters to avoid optical saturation [29], was launched into the discharge chamber, passed parallel to the electrodes, and was detected on the opposite side of the chamber with the photodiode PD3 (figure 1). In steady-state studies, all three signals from PDs were simultaneously recorded and averaged in different channels of a digital oscilloscope and then treated by a computer. In time resolved studies, the signal from PD2 is used to set the laser frequency at the centre of the absorption line, where the maximum absorption is reached, and the signal from PD3 is averaged on the digital oscilloscope, triggered synchronously with the RF discharge, and hence recorded in the computer.

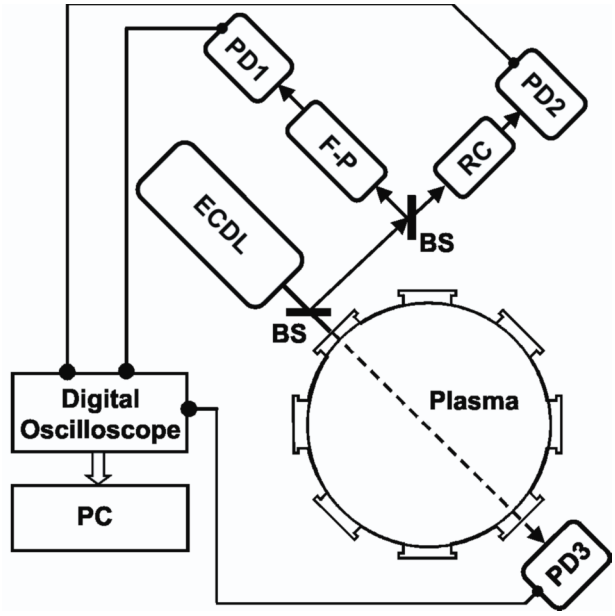

Figure1. Experimental set-up, top view. ECDL - External Cavity Diode Laser, F-P - Fabry-Perot etalon, RC - reference cell (low pressure low current Ar discharge), BS - Beam Splitters, PD1, 2, 3 - Photodiodes.

3. Results and discussion

3.1. Gas temperature

Laser absorption spectroscopy is based on Beer-Lambert's law, which in low pressure and low density plasmas, when the Doppler Broadening controls the line-shape, writes [29]:

$$\ln\left(\frac{I_0(\nu)}{I(\nu)}\right) = \frac{g_u}{g_l}\frac{\lambda_0^2}{8\pi} A_{\mathrm{ul}}\, l_{\mathrm{eff}}\, N \frac{2\sqrt{\ln(2)/\pi}}{\delta\nu_{\mathrm{D}}} \exp\left(-4\ln(2)\frac{(\nu-\nu_0)^2}{(\delta\nu_{\mathrm{D}})^2}\right) \qquad (1)$$

where $I_0(\nu)/I(\nu)$ are the detected intensity at frequency ν without and with absorbing atoms, A_{ul}=5.18 10^6 s^{-1} is the emission Einstein's coefficient of the λ_0 =772.38 nm argon line [27], g_u=3 and g_l=5 are the statistical weights of the upper and lower levels of the line, respectively, N is the densities of absorbing atoms, l_{eff}=30 cm is the effective absorption length (diameter of the electrodes) and $\delta\nu_{\mathrm{D}}$ is the Doppler width of the line given by [29]:

$$\delta\nu_{\mathrm{D}}(Hz) = (2\nu_0/c)\sqrt{2\ln 2(RT_{\mathrm{g}}/M)} = 7.16\cdot 10^{-7}\nu_0\sqrt{T_{\mathrm{g}}/M} \qquad (2)$$

When the laser frequency is set at the line centre ν_0, the density of Ar*($^3P_2$) atoms can be deduced from the measured ratio of I_0/I, if the Doppler width, which depends on T_g, is known and assuming homogeneous density in radial direction:

$$[Ar^*(^3P_2)] = \frac{g_l \, 4\pi \, \delta\nu_D}{g_u \, \lambda_0^2 \, l_{eff} \, \sqrt{\ln(2)/\pi} \, \ln(I_0/I)} \quad (3)$$

For T_g measurements, the plasma is run in continuous regime and the laser frequency is scanned at about 25 Hz around the line centre. Figure 2 shows as an example, the absorption line profile and the F-P transmission signal, after the time scale of the oscilloscope has been converted to GHz by means of F-P peaks, separated by 0.375 GHz. In pure argon, T_g values deduced from the fit are 293 K and 295 K at 15 W and 50 W of RF power, respectively. Considering the ±10 K estimated uncertainty on these values, we conclude that in pure argon plasma the gas remains at room temperature. When the laser beam was moved close to the electrode (inside the sheath or in the negative glow) the measured T_g corresponded also to the room temperature. In argon with the presence of dust (4: Ar/dust) we have measured 333 K and 365 K at 15 W and 50 W of RF power, respectively. These values are 10% and 20% higher than the room temperature. But close to the electrodes, T_g was found to be 306 K and 320 K at 15 W and 50 W, respectively. We believe that, this small increase of T_g in the plasma bulk after dust particles are formed is due to the increase of the plasma electric field by an order of magnitude, as was reported in [9]. This induces an enhancement of the kinetic energy of ions in the bulk of the discharge. Part of this energy is transferred to argon atoms in charge exchange and elastic collisions. But near the electrodes, the gas remains in equilibrium with electrodes which are at room temperature.

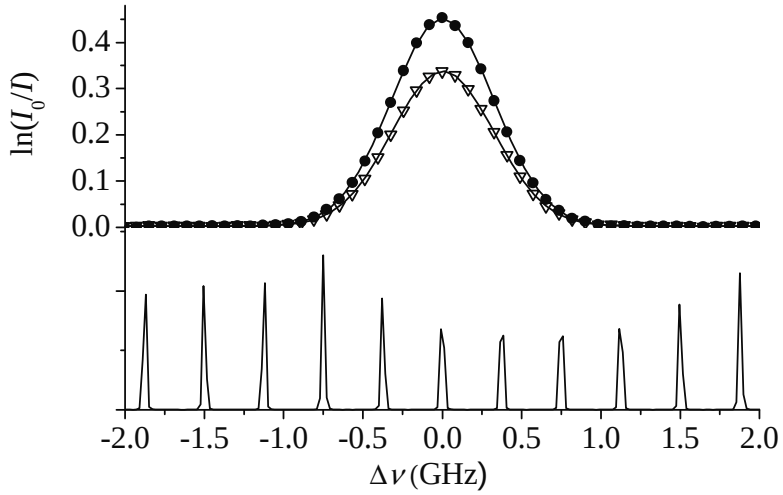

Figure 2. Fabry-Perot transmission signal with 0.375 GHz peak separation (lower part) and absorption line profile at two different discharge powers of pure argon plasma: 15 W (triangles) and 50 W (solid circles). Gaussian fits to experimental points (solid lines) provides the gas temperature (T_g) and metastable density (N_m): $N_m = 1.22\times10^{16}$ m^{-3}, T_g = 293 K at 15 W and $N_m = 1.65\times10^{16}$ m^{-3}, T_g = 295 K, 50 W.

3.2. Time dependent Ar density*

Figure 3 shows the time variation of Ar* ($^3P_2$) metastable density at the middle of the electrodes for different gas composition and at 20 W and 80 W applied RF powers. The RF modulation frequency was around 100 Hz, with 50% duty cycle. Reported densities are deduced from (3), assuming T_g= 300 K. They therefore could be underestimated at maximum by 10% in dusty plasmas. We observe that in all cases the steady-state density is reached at about 1 ms after the plasma ignition (at t = 0). We will first discuss the variation of these steady-state density with plasma parameter and hence analyze changes induced by these parameters on the lifetime of Ar* atoms in the afterglow.

3.2.1. Steady-state density. Under our experimental conditions, the main production mechanism of metastable atoms is the direct electron-impact excitation from the ground state argon atom. The steady state density results therefore from an equilibrium between production and loss frequencies of Ar* atoms [30]:

$$[\mathrm{Ar}^*] = k_e(T_e).n_e.[\mathrm{Ar}]\tau \quad (4)$$

where k_e is the electron temperature (T_e) dependent excitation rate, n_e the electron density, [Ar] argon density and τ the lifetime of metastable atoms, which can have some n_e and T_e dependence [28,30].

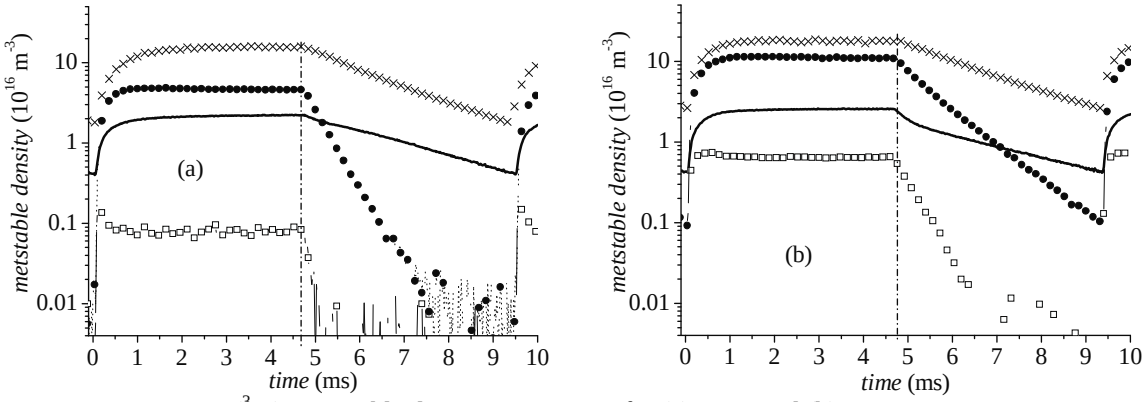

Figure 3. Ar* ($^3P_2$) metastable density versus time for (a) 20 W and (b) 80 W input powers. Different lines/symbols are for different gas mixtures: solid line – pure Ar; open squares – Ar/C_2H_2; solid circles – Ar/C_2H_2/dust; crosses – Ar/dust. The vertical dot-dashed line indicates the OFF time of the RF power.

In pure argon, the steady-state Ar* density is about 2 10^{16} m^{-3} at 20 W and only slightly increases with RF power at 80 W. As n_e should increase linearly with power, we can conclude that the enhancement of excitation frequency is almost compensated by a decay of the lifetime of Ar* atoms by electron impact de-excitation of these atoms [30].

With acetylene added to the feed gas (Ar/C_2H_2 graphs in figure 3), Ar* density falls to 1 10^{15} m^{-3} at 20 W. This decrease by a factor of 20 can be attributed to the efficient quenching of Ar* atoms by C_2H_2, for which the measured quenching rate coefficient is k_q=5.6 10^{-16} m^{3}s^{-1} [31]. However, considering the respective flow rates 8 sccm and 0.5 sccm for Ar and C_2H_2 and the 0.1 mbar total pressure, the estimated density of C_2H_2 would be 1.5 10^{20} m^{-3}, which should result in a quenching frequency of Ar* by C_2H_2 of $\nu_q \approx 8\ 10^4$ s^{-1}. As it will be discussed in the next section, the corresponding 12 μs lifetime is more than 2 orders of magnitude smaller than the measured lifetime of Ar* in pure argon. Hence considering that adding C_2H_2 can not introduce an important enhancement of n_e and T_e, according to (4) the effective decrease in Ar* density should be even larger. We believe that due to the high degree of dissociation of C_2H_2 by the discharge, its density in the plasma bulk is much lower than the estimated value from relative flow rates and pressure. At 80 W, the Ar* density is reduced by only a factor of 4 when C_2H_2 is added to argon. In fact, the degree of dissociation of acetylene increases with RF power.

After dust particles are formed in Ar/acetylene discharge (Ar/C_2H_2/dust graphs in figure 3), Ar* density increases significantly and even overpasses its value in pure argon. This important enhancement has several origins. First, in the presence of dust particles the plasma becomes more resistive and the RF power dissipated in the bulk increases [9,12]. Second, the excitation zone which was near the electrodes in the wave riding α mode, becomes more homogeneous with dusts [11,13]. So increasing the Ar* production term in the halfway from electrodes, where data shown in figure 3 have been taken. Finally, with higher T_e in dusty plasma, the degree of dissociation of C_2H_2 becomes larger, hence inducing an enhancement of the lifetime of Ar* atoms. Close to the electrode (data not shown), the rise of Ar* density with dust is much less spectacular than in the plasma centre.

Stopping the C_2H_2 flow leaves dust particles in the plasma and induces further rise of Ar* density (Ar/dust graphs in figure 3). In fact, Ar* is no more quenched by C_2H_2 and its lifetime increases. As expected, this rise is more pronounced in 20W plasma than in 80W plasma because C_2H_2 was less dissociated in the former case. Measured densities in argon with dust are almost an order of magnitude larger than in pure argon. The origin of this large difference relays on the enhancement of T_e combined to the spatially homogeneous excitation of Ar* atoms in γ' regime, associated to the presence of dust, whereas in pure argon the excitation zone is localized near the electrodes, α regime [11].

3.2.2. Lifetime in the afterglow. After the RF plasma is switched off, production of Ar* atoms stops and their density decays almost exponentially by diffusion to the electrodes and by reaction in the plasma volume with other particles.

In pure argon, using the diffusion coefficient of Ar* atoms in Ar D_0.[Ar]=1.8 10^{20} $m^{-1}s^{-1}$ [28] and considering our experimental conditions, the loss frequency of Ar* by diffusion to the electrodes is ν_d=150 s^{-1}. At 0.1 mbar, loss frequencies by two and three body collisions with argon are 5 s^{-1} and 1 s^{-1}, respectively [28], hence negligible. The lifetime deduced from decay curves of Fig. 3 is about 3.4 ms, indicating the presence of a small amount of impurity (probably C_2H_2 trace left in the reactor chamber).

The very fast decay of Ar* density when acetylene is added to the feed gas results from its quenching by C_2H_2. However, the measured lifetimes, about 200 and 500 µs at 20 W and 80 W, respectively, are much larger than the expected 12 µs with the amount of C_2H_2 introduced into the chamber. This proves that in the plasma volume, the dissociation rate of C_2H_2 is about 95% at 20 W and approaches 98% at 80 W.

After the apparition of dust particles, the lifetime increases up to about 1.2 ms at 80 W and it is again larger than at 20 W. This large lifetime indicates that in the bulk plasma C_2H_2 is dissociated to about 99%. The enhancement of the electron temperature should cause the observed high degree of dissociation of acetylene.

With C_2H_2 stopped and dust particles remained in the discharge (Ar/dust), the lifetime reaches almost its value in pure argon, remaining however always slightly lower. This lower value could either be due to the lost of Ar* atoms on dust particles or to quenching by small amount of carbonated molecules desorbed from reactor walls and electrodes. To rule out the first possibility, we can estimate the related loss frequency, ν_D, assuming a density N_D=1 10^{12} m^{-3} of dust particles of 30 nm radius. These are the characteristic values measured by light scattering in our reactor and working conditions [32] and would correspond to a surface of about S_D=1 10^{-14} m^2 for each particle. A rough calculation, assuming that the number of atoms of mean velocity w impinging on a surface s is 1/4×N×<w>s, would provide:

$$\nu_D = (1/4) < w_{Ar^*} > N_D S_D \cong 1 s^{-1} \qquad (5)$$

where $<w_{Ar^*}>$=400 m/s is the mean velocity of Ar* atoms impinging on dust particles. In fact, this loss frequency on dust is much smaller than the loss by diffusion, ν_d=150 s^{-1} and is hence negligible. Do *et al* [21] have observed the quenching of Ne* metastable atoms in the sheath boundary, where dust particles were concentrated. However, in that work, if the density of dust particles were comparable to ours, the 10 µm size of their SiO_2 particles corresponds to more than 4 orders of magnitude larger surface, highlighting the influence of dust particles on quenching of Ne* atoms.

An important point that we would like to point out is the faster decay of Ar* metastable atoms in the few 100s of µs following the end of the discharge in 80 W pure argon (Ar graph in Fig. 3b). Almost absent in the 20 W pure argon plasma, this early fast decay is also missing in the 80 W Ar/dust plasma. We attribute this decay to the quenching of Ar* atoms by plasma electrons, which in fact transfer Ar* metastables to the Ar* ($^3P_1$) resonant state (for more detail see refs. 26 and 28):

$$Ar^*(^3P_2) + e \rightarrow Ar^*(^3P_1) + e \qquad (6)$$

This reaction is endoergic by only 75 meV and can be very efficient in the early afterglow. For T_e above 0.2 eV, the reported rate coefficient of k_t=2 10^{-13} $m^3.s^{-1}$ [28,30] would correspond to a decay frequency of ν_t=1000 s^{-1} for n_e= 5 10^{15} m^{-3}. In reality, due to the radiation trapping in large size plasmas, the density of atoms in the $^3P_1$ resonance state remains high and the reverse process of (6) brings back to the Ar*($^3P_2$) metastable state a part of the transferred atoms. As a consequence, the overall rate coefficient of electron impact quenching of Ar*($^3P_2$) atoms is reduced to a few times 10^{-14} m^3s^{-1} (see [30] for discussion), resulting in a decay frequency of a few hundreds s^{-1}, comparable to the decay frequency of Ar* by diffusion. In the pure argon 80 W plasma the above mentioned n_e is reached [33] but in 20 W plasma n_e is about 4 times smaller and an order of magnitude smaller in the presence of dust particles [32-34]. Consequently, the effective depopulation of Ar*($^3P_2$) state by electrons will

be negligible in these later cases.

4. Conclusion

In this work, we have shown that Ar*($^3P_2$) density can be an excellent probe of dust formation in argon/acetylene plasmas. Due to the enhancement of the electron temperature and the change of discharge from α regime to γ' regime after dust formation in the plasma, the steady-state population of Ar*($^3P_2$) metastable state becomes an order of magnitude larger in dusty argon plasma than in pure argon discharge. Measured decay times of metastable atoms in the afterglow indicate that C_2H_2 is highly dissociated in the plasma volume, its degree of dissociation reaching 99% at 80 W argon/acetylene discharges` after powder formation. Our results also show the depopulation in the early afterglow of metastable state by electron impact transfer to the resonant Ar*($^3P_1$) state. But under our experimental conditions, the quenching of metastable atoms on the surface of dust particles can be neglected.

Acknowledgments

This work was supported by the DFG through Project No. WI 1700/3-1, Graduierten Kolleg 1051 and Research Department “Plasma with Complex Interactions”, Ruhr Universität Bochum.

References

[1] See a comprehensive study of dusty plasma basics and application in 1999 *Dusty Plasmas: Physics, Chemistry, and Technological Impacts in Plasma Processing*, ed A Bouchoule (New York: Wiley)
[2] Boufendi L, Bouchoule A and Hibid T 1996 *J. Vac. Sci. Technol.* A. **14** 572
[3] Hollenstein Ch 2000 *Plasma Phys. Control. Fusion* **42** R93
[4] Stoffels E, Stoffels W W, Kersten H, Swinkels G H P M and Kroesen G M W 2001 *Phys. Scr.* **T89** 168
[5] Samsonov D and Goree J 1999 *Phys. Rev.* E **59** 1047
Samsonov D and Goree J 1999 *IEEE Trans. Plasma Sci.* **27** 76
[6] Stefanović I, Kovačević E, Berndt J and Winter J 2003 *NJP* **5** 39
[7] Bouchoule A and Boufendi L 1994 *Plasma Sources Sci. Technol.* **3** 292
[8] Schauer J C, Hong S and J. Winter 2004 *Plasma Sources Sci. Technol.* **13** 636
[9] Belenguer Ph, Blondeau J Ph, Boufendi L, Toogood T, Plain A, Bouchoule A, Laure C, and Boeuf J P 1992 *Phys. Rev.* A **46** 7923
[10] Perrin J, Böhm Ch, Etemadi R and Lioret A 1994 *Plasma Sources Sci. Technol.* **3** 252
[11] Denysenko I, Yu M Y, Ostrikov K, Azarenkov N A, and Stenflo L 2004 *Phys. Plasmas* **11** 4959
[12] Denysenko I, Berndt J, Kovačević E, Stefanović I, Selenin V and Winter J 2006 *Phys. of Plasmas* **13** 073507
[13] Schweigert I V, Alexandrov A L, Ariskin D A, Peeters F M, Stefanović I, Kovačević E, Berndt J and Winter J 2008 *Phys. Rev. E* **78** 026410
[14] Tochikubo F, Petrović Z Lj, Kakuta S, Nakano N and Makabe T 1994 *Jpn. J. Appl. Phys.* **33** 4271
[15] Moshkalyov S M, Steen P G, Gomez S and Graham W 1999 *Appl. Phys. Lett.* **75** 328
[16] Siefert S, Sands B L and Ganguly B N 2006 *Appl. Phys. Lett.* **89** 011502
[17] Baguer N, Bogaerts A, Donko Z, Gijbels R and Sadeghi N 2005 *J. Appl. Phys.* **97** 123305
[18] Cunge G, Ramos R, Vempaire D, Touzeau M, Nejbauer M and Sadeghi N 2009 *J. Vac. Sci. Technol. A.* **27** 471
[19] Engeln R, Mazouffre S, Vankan P, Schram D C and Sadeghi N 2001 *Plasma Sources Sci. Technol.* **10** 595
[20] Clarenbach B, Lorenz B, Krämer M and Sadeghi N 2003 *Plasma Sources Sci. Technol.* **12** 345
[21] Do H T, Kersten H and Hippler R 2008 *NJP* **10** 053010
[22] Do H T, Sushkov V and Hippler R 2009 *NJP* **11** 033020
[23] Howling A A, Dorier J-L and Hollenstein Ch 1993 *Appl. Phys. Lett.* **62** 1341
[24] Winter J, Berndt J, Hong S-H, Kovačević E, Stefanović I and Stepanović O 2009 *Plasma Sources Sci. Technol.* **18** 034010
[25] Kovačević E, Stefanović I, Berndt J and Winter J 2003 *J. Appl. Phys* **93** 2924.

[26] Hong S-H, Berndt J and Winter J 2003 *Plasma Sources Sci. Technol.* **12** 46
[27] W. L. Wiese, J. W. Brault, K. Danzmann, V. Helbig and M. Kock, Phys. Rev. A **39** (1989) 2461
[28] O'Connell D, Gans T, Crintea D L, Czarnetzki U and Sadeghi N 2008 *J. Phys. D: Appl. Phys.* **41** 035208
[29] Sadeghi N 2005 *Journal of Plasma and Fusion Research*, **80** 767
[30] Latrasse L, Sadeghi N, Lacoste A, Bes A and Pelletier J 2007 *J. Phys. D: Appl. Phys.* **40** 5177
[31] Velazco J E, Kolts J H and Setser D W 1978 *J. Chem. Phys.* **69** 4358
[32] Stefanović I, Berndt J, Marić D, Šamara V, Radmilović-Radjenović M, Petrović Z Lj, Kovačević E and Winter J 2006 *Phys. Rev.* E **74** 024606
[33] Stefanović I, *et al*. will be published
[34] Berndt J, Kovačević E, Selenin V, Stefanović I and Winter J 2006 *Plasma Sources Sci. Technol.* **15** 18